Batteries & Supercaps

Research Article
doi.org/10.1002/batt.202400462

Chemistry Europe
European Chemical Societies Publishing

www.batteries-supercaps.org

Artificial Solid Electrolyte Interface Securing the Reversible Deposition of Lithium for High Performance Lithium Batteries

Xuanyi Chen[+],[a] Kaiji Lin[+],[a] Mengxue Wu,[a] Yuyuan Li,[a] Zhichuan Shen,[a] Naiguang Wang,[a] Yan Sun,*[b] Chunsheng Li,[b] Jiahong Pan,[c] Abdullah N. Alodhayb,*[d] and Zhicong Shi*[a, e]

Lithium batteries (LBs) are among the most promising energy storage devices due to their high theoretical energy density. However, Li dendrites, which may grow in an uncontrolled manner during cycling, can puncture the electrolyte in LBs and cause a short circuit and thermal runaway. In this study, by using a simple coating process, a new type of organic/inorganic composite protective layer is constructed on a current collector by scraping PVDF and Li_3PO_4 particles on the surface of a copper foil. The prepared composite coating shows excellent mechanical and electrochemical properties, and the ability to maintain a stable coulombic efficiency of 98% for lithium deposition and dissolution at 0.5 mA cm^{-2}. This paper describes the mechanism of action of the prepared composite anode and proposes further improvements of the electrode.

Introduction

As portable electronics and electric vehicles have been increasingly integrated into our daily lives, the demand for high-power, energy-intensive batteries has increased dramatically.[1–3] However, because of the uneven deposition of lithium ions and the uncontrolled growth of dendrites[4], battery membranes can be easily perforated, leading to short circuits, fires, and even explosions.[5–8] To satisfy the increasing energy needs associated with society's development, there is an urgent need to develop new battery materials to improve the energy density and safety performance of batteries.[9–11] Generally, artificial SEIs are categorized into organic and inorganic types.[12] Organic polymers, with their inherent viscosity and semi-liquid properties, are well-suited for direct application on alkali metal surfaces to create dense SEI films. These attributes endow the polymer SEI with excellent wettability for both alkali metals and solid electrolytes, offering distinct advantages in solid-state batteries. to enhance their interfacial contact. Moreover, the elasticity of polymers effectively accommodates the volume changes during the lithium deposition process. Zhang et al.[13] prepared an artificial SEI using agarose (AG). The agarose polymer combines rigidity with flexibility, allowing lithiumions in the electrolyte to diffuse through the agarose membrane and uniformly deposit on copper foil to form a lithium metal layer, thereby inhibiting the growth of lithium dendrites. The agarose-modified electrode also demonstrates a reduced lithium nucleation overpotential, effectively mitigating interfacial side reactions, and substantially enhancing overall battery performance. However, SEIs based on organic polymers typically depend on their inherent elasticity and the strength of bonding between functional groups and lithium salts to manage the state of lithium ion deposition, and they still lack mechanical strength and rigidity.[14,15]

To solve the abovementioned problems, a method to achieve uniform deposition and controlled growth of alkali metals via the lithiophilic modification of a current collector and the construction of an artificial solid electrolyte interface (SEI) is described in this article.

Lithiophilic modification of a copper foil surface can effectively improve the deposition and nucleation of lithium ions, but the thick lithium metal layer and an excessive SEI film inhibit the performance of lithiophilic substances at a high current density and circulation capacity. The formation of a protective layer on a copper foil to induce lithium deposition between the copper foil and the protective layer can effectively prevent direct contact between lithium metal and the electrolyte, and then stabilize the lithium ion flux. The ideal artificial SEI protective layer usually has good lithium ion conductivity, a good electrolyte infiltration rate, excellent stability, and excellent mechanical strength.[16,17]

[a] X. Chen,[+] K. Lin,[+] M. Wu, Y. Li, Z. Shen, N. Wang, Z. Shi
Institute of Batteries, School of Materials and Energy, Guangdong University of Technology, Guangzhou 510006, China
E-mail: zhicong@gdut.edu.cn

[b] Y. Sun, C. Li
Key Laboratory of Advanced Electrode Materials for Novel Solar Cells for Petroleum and Chemical Industry of China, School of Chemistry and Life Sciences, Suzhou University of Science and Technology, Suzhou City 215009, China
E-mail: juzi14@163.com

[c] J. Pan
State Key Laboratory of Featured Metal Materials and Life-Cycle Safety for Composite Structures, School of Resources, Environments and Materials, Guangxi University, Nanning 530004, China

[d] A. N. Alodhayb
King Abdullah Institute for Nanotechnology, King Saud University, Riyadh 11451, Saudi Arabia
E-mail: aalodhayb@ksu.edu.sa

[e] Z. Shi
Key Laboratory of Advanced Energy Materials Chemistry (Ministry of Education), Nankai University, Tianjin 300071, China

[+] These authors contributed equally to this work.

Research Article
doi.org/10.1002/batt.202400462
Chemistry Europe
European Chemical Societies Publishing

Polyvinylidene difluoride (PVDF), a common binder for lithium ion batteries (LIBs), is a homopolymer with a high dielectric constant and good stability and film-forming properties, but its low mechanical strength makes it difficult to satisfy the requirements for the formation of an artificial SEI. Li_3PO_4 (LPO) has a high elastic modulus (10–11 GPa) and ionic conductivity, and it can be combined with PVDF to form a stable interface to improve the electrochemical performance of LIBs.[18–20]

In this study, a simple coating process was used to scrape PVDF and Li_3PO_4 particles onto the surface of a copper foil to allow loading of an artificial SEI protective layer onto the copper foil. The PVDF matrix maintained the mechanical integrity and chemical stability of the composite during cycling, and the Li_3PO_4 particles provided an efficient channel for lithium ion diffusion. The organic/inorganic composite coating composed of both materials was used to regulate the deposition of lithium ions and prevent side reactions between the electrolyte and lithium metal. The prepared PVDF-LPO@Cu/Li achieved stable deposition/stripping of lithium metal and exhibited better electrochemical performance under lithium-poor conditions.

Experimental Section

Preparation of PVDF-LPO@Cu

First, 0.4 g of PVDF powder was weighed and dissolved in 10 g of *N*-methyl-2-pyrrolidone (NMP). Then, 0.5 g of Li_3PO_4 powder was added, and the mixture was stirred well. Finally, a 50 μm scraper was used to scrape the material onto a copper foil.

Preparation of a PVDF-LPO@Cu/Lithium Metal Composite Anode

A PVDF-LPO@Cu||Li battery was assembled, and 1 mAh cm^{-2} lithium was electrodeposited on the surface of Cu at a current density of 1 mA cm^{-2}; then, the battery was disassembled in a glove box and cleaned by dimethyl carbonate to obtain a PVDF-LPO@Cu/Li composite anode.

Preparation of a Lithium Iron Phosphate (LFP) Cathode Sheet

LFP, conductive carbon black, and PVDF were mixed and scraped onto a carbonized aluminum foil at a mass ratio of 8:1:1. The resulting sample was pressed into a 10 mm round sheet after vacuum drying.

Battery Assembly

A half battery is composed of a copper foil cathode and a lithium metal anode. A full battery is composed of an LFP cathode and a Cu/Li anode or a PVDF-LPO@Cu/Li anode. The electrolyte was 1 M lithium bis(trifluoromethanesulfonyl)imide (LiTFSI) dissolved in dimethyl ether and dioxolane (DOL) with 2 wt.% $LiNO_3$.

Results and Discussion

Physical Properties of PVDF-LPO@Cu

The scanning electron microscopy (SEM) images shown in Figure 1 compare two types of current collectors, namely, copper foil (bare Cu) and the prepared PVDF-LPO@Cu. The image in Figure 1(a) shows the smooth surface of bare Cu. Figure 1(b) shows images of Li_3PO_4 particles of various sizes embedded in PVDF and coated onto the surface of a copper foil, forming an organic/inorganic composite SEI protective layer. A comparison between Figure 1(b) and (a) indicates that PVDF-LPO was relatively uniformly and densely coated on the copper surface.

In the X-ray diffraction (XRD) pattern of PVDF-LPO@Cu (Figure 2), the peaks at 43.3°, 50.4°, and 74.1° correspond to the (111), (200), and (220) crystal planes of copper (PDF# 85–1326).[21] The peaks at 50.4° and 74.1° correspond to the (012) and (110) crystal planes of Li_3PO_4 (PDF#84–0003). These findings indicate the presence of lithium phosphate particles.

Figure 3 shows the C 1s, F 1s, and P 2p X-ray photoelectron spectroscopy (XPS) results for PVDF-LPO@Cu. As shown in Figure 3, the C 1s spectrum of PVDF-LPO@Cu was fitted with four peaks corresponding to the following structural components: C–H at 283.4 eV, CH_2 at 284.8 eV, C=O at 286.6 eV, and CF_2 at 289.3 eV. The peak area ratio of CH_2 to CF_2 was approximately 1:1, consistent with the structure of PVDF. In addition, C=O was primarily formed by the oxidation of part of

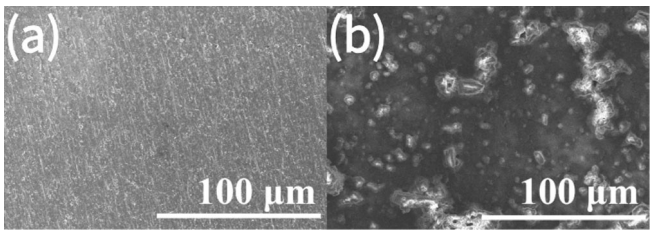

Figure 1. SEM images of bare Cu (a) and PVDF-LPO@Cu (b).

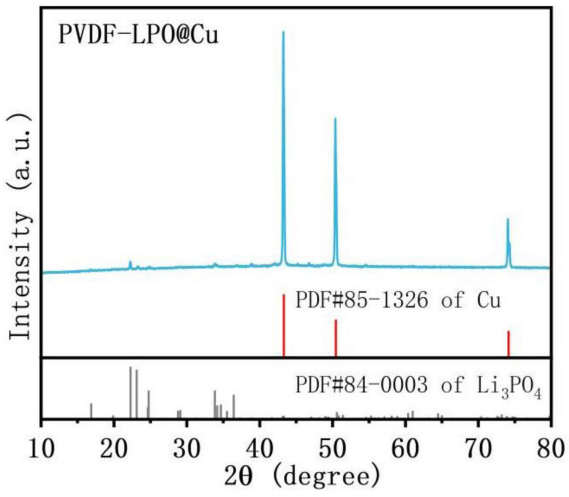

Figure 2. XRD pattern of PVDF-LPO@Cu.

Research Article
doi.org/10.1002/batt.202400462
Chemistry Europe
European Chemical Societies Publishing

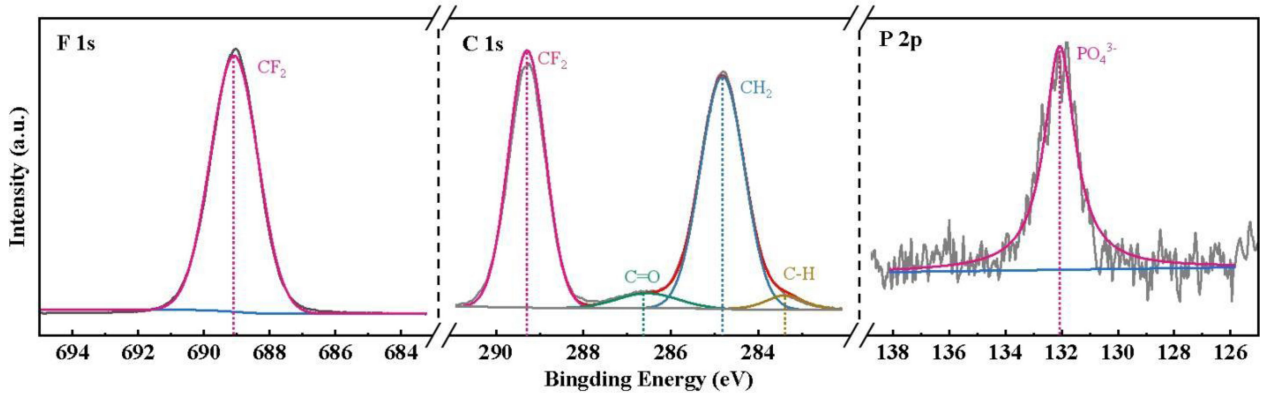

Figure 3. C 1s, F 1s, and P 2p XPS patterns of PVDF-LPO@Cu.

the carbon chain. The peak at 685.15 eV in the F1s spectrum was attributed to CF_2, further confirming the presence of PVDF.[22] The peak at 132.15 eV in the P 2p spectrum of PVDF-LPO was attributed to PO_4^{3-}, proving that the synthetic coating contained Li_3PO_4.[23]

Electrochemical Properties of the Prepared PVDF-LPO@Cu/Li Composite Anode

To assemble a full battery, 1 mAh cm^{-2} lithium metal was deposited on a copper foil or a PVDF-LPO@Cu, coupled with an LFP cathode. In the first cycle, the discharge capacity and coulombic efficiency of the LFP||bare Cu/Li battery at 0.2 C were 154.5 mAh g^{-1} and 95.13% in Figure 4(c), respectively, similar to those of the LFP||PVDF-LPO@Cu/Li battery (157.4 mAh g^{-1} and 94.59% in Figure 4(b)).

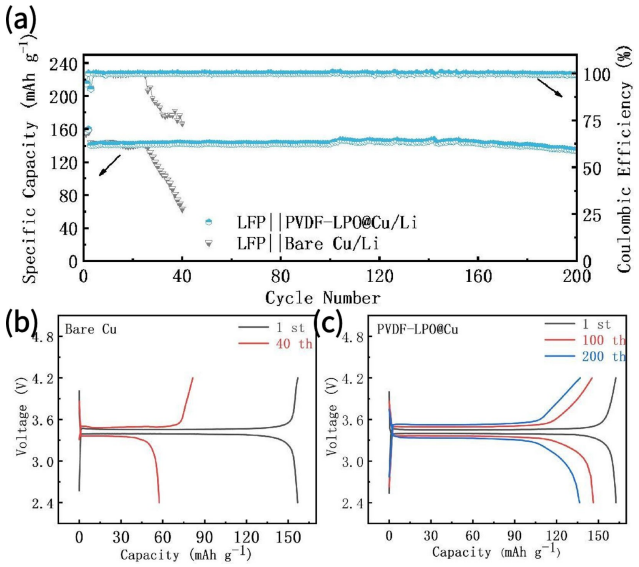

Figure 4. Electrochemical cycle performance of LFP||bare Cu/Li and LFP||PVDF-LPO@Cu/Li (a). Charge and discharge curves of the 1st and 40th cycles of LFP||bare Cu/Li (b). Charge and discharge curves for the 1st, 100th and 200th cycles of LFP||PVDF-LPO@Cu/Li (c).

In subsequent cycles, the discharge capacity of the LFP||bare Cu/Li battery began to decline rapidly after approximately 30 cycles, and the coulombic efficiency was also unstable (Figure 4a). The performance of the LFP||bare Cu/Li battery declined rapidly because of the rapid consumption of lithium under lithium-poor conditions, resulting in dead lithium and the loss of lithium inside the battery.[24]

In contrast, the LFP||PVDF-LPO@Cu/Li battery maintained stable cycling for 200 cycles (Figure 4a). Its discharge capacity remained at 140 mAh g^{-1} over an extended period, and the coulombic efficiency was also maintained at approximately 100%. The protective layer formed by the combination of PVDF and lithium phosphate promoted the generation of LiF and formed a buffer layer to effectively reduce the occurrence of side reactions at the interface and to balance the stress caused by morphological changes, thus allowing homogeneous lithium ion deposition and preventing the growth of lithium dendrites.

Mechanism Analysis of the PVDF-LPO@Cu/Li Composite Anode

The excellent electrochemical performance exhibited by the full battery can be explained by the deposition state of the lithium metal on the copper foil. A copper foil and lithium metal half cell assembly was used for the electrochemical deposition and stripping experiments. At 1 mA cm^{-2}, the nucleation overpotential of bare Cu was 94.2 mV, while that of PVDF-LPO@Cu was slightly higher (109.1 mV) because the ion transport channel of the PVDF-LPO protective layer remained closed. Thus, lithium ions required higher energy to pass through the protective layer (Figure 5(a)). The nucleation potential of lithium on PVDF-LPO@Cu was lower than that of bare Cu foil after deposition of lithium at 0.5 mAh cm^{-2}. The nucleation potential of lithium on bare Cu foil decreased to 47.4 mV after deposition of lithium at 2 mAh cm^{-2}, while it decreased to 43.1 mV for the PVDF-LPO@Cu foil. A lower lithium nucleation potential indicates a lower nucleation barrier, corresponding to the improved lithium ion transport and interface stability. During subsequent stripping, the coulombic efficiency of lithium deposition on bare Cu foil reached 85.64%, while that of PVDF-LPO@Cu foil reached

Research Article
doi.org/10.1002/batt.202400462
Chemistry Europe
European Chemical Societies Publishing

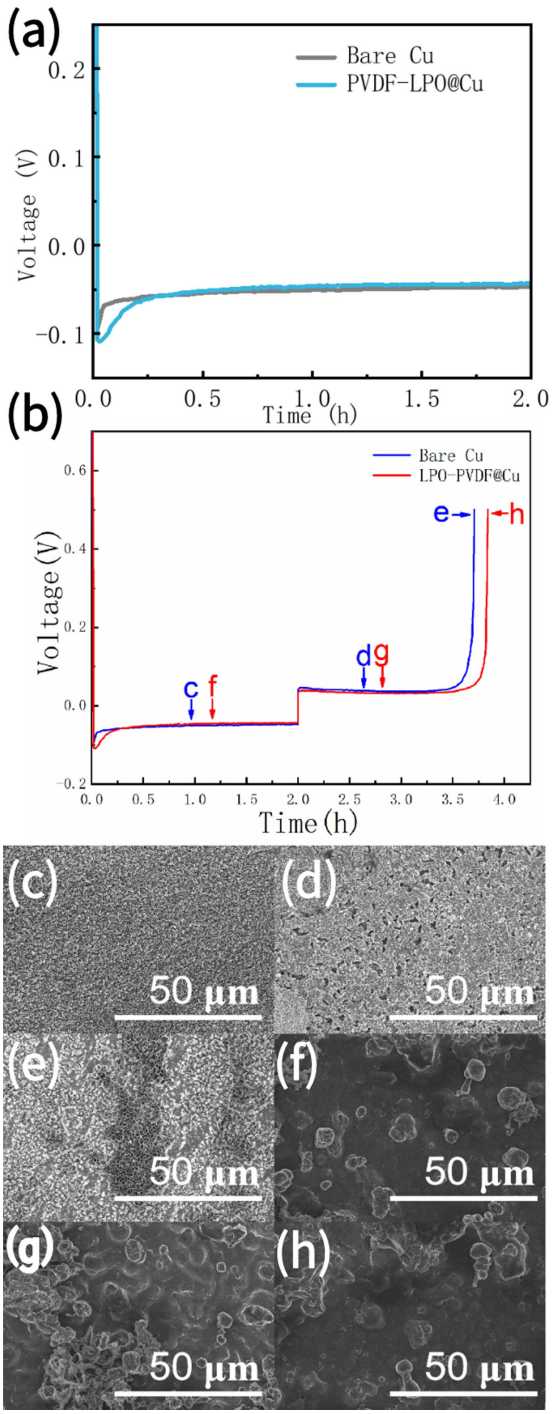

Figure 5. Voltage profiles of bare Cu and PVDF-LPO@Cu for lithium deposition at 1 mA cm^{-2} (a), charge/discharge profiles of bare Cu and PVDF-LPO@Cu at 1 mA cm^{-2} (b), and SEM images of bare Cu and PVDF-LPO@Cu at indicated positions corresponding to the charge/discharge profiles (c–h).

91.9%. After deposition and stripping of lithium at 1 mAh cm^{-2}, the SEM images of bare Cu and PVDF-LPO@Cu showed that many small particles were closely distributed on the surface of bare Cu foil, while some micron-sized particles were observed on the surface of PVDF-LPO@Cu foil. After further deposition of lithium at 2 mAh cm^{-2} and stripping at 1 mAh cm^{-2}, the surface of bare Cu foil exhibited many holes caused by the uneven dissolution of lithium metal during stripping, while the surface of PVDF-LPO@Cu foil remained similar before and after stripping.

When the lithium on the copper foil was completely stripped until the voltage increased to 0.5 V, the byproducts generated by the reaction between lithium metal and the electrolyte remained on the surface of bare Cu foil, whereas the PVDF-LPO@Cu foil surface did not undergo significant changes. The PVDF-LPO protective layer effectively prevented side reactions at the interface, allowing the battery to work more efficiently and stably. Figure 6 shows an enlarged SEM image of lithium after stripping. The lithium deposited on the bare Cu foil surface after stripping of lithium at 1 mAh cm^{-2} was spherical, with a diameter of approximately 1 μm, and some bumpiness was observed as a result of preferential stripping at certain sites. After stripping at 0.5 V, the surface of the copper foil had a considerable amount of a flocculent material that was originally wrapped in the spherical lithium metal structure. However, PVDF-LPO@Cu foil did not change considerably, except for a few particles.

The above results show that the PVDF-LPO@Cu current collector formed a more stable SEI in the presence of PVDF and the lithium phosphate composite protective layer, allowing the lithium metal deposited under the SEI to effectively prevent side reactions between lithium metal and the electrolyte.

XPS was used to determine the composition of the SEI and the surface of the current collector. The XPS spectrum in Figure 7 shows the elemental composition on the surface of the two current collectors. The surface elements of bare Cu foil were mainly lithium and oxygen, which were derived from lithium metal deposited and oxidized on the current collector. In addition, there were also trace amounts of carbon and fluorine on this surface, which were attributed to the electrolyte and side reaction with lithium. In contrast, the surface of PVDF-LPO@Cu foil contained mainly oxygen and fluorine, with a small amount of carbon and lithium. Notably, the fluorine and carbon contents on the PVDF-LPO@Cu foil surface were significantly greater than those on bare Cu foil, mostly because of the initial PVDF on the current collector surface, while a small portion

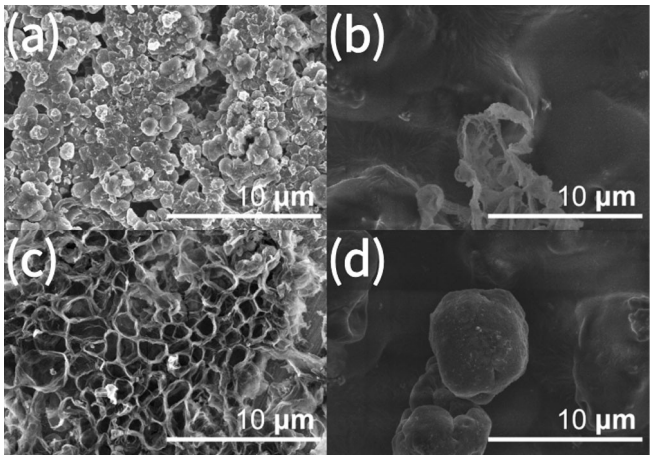

Figure 6. Magnified SEM images of bare Cu (a, c) and PVDF-LPO@Cu (b, d) after lithium deposition.

Research Article
doi.org/10.1002/batt.202400462
Chemistry Europe
European Chemical Societies Publishing

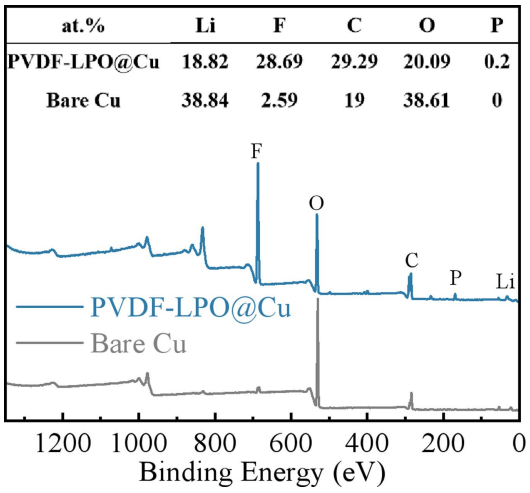

Figure 7. XPS spectra of bare Cu and PVDF-LPO@Cu after lithium deposition; the inset shows a table listing the elemental composition of the SEI.

originated from the reduction and decomposition of the electrolyte.

Figure 8 shows the XPS spectra of bare Cu and PVDF-LPO@Cu foils. The Li 1s spectra were each deconvoluted into three peaks located at ~54.65 eV, ~55.4 eV, and ~56 eV, corresponding to Li_2O, Li_2CO_3, and LiF respectively.[22,24,25] As seen by comparing the two spectra, it contained a much larger proportion of Li_2O than of LiF and Li_2CO_3 for bare Cu foil, while it had similar proportions of these three compounds on the surface of PVDF-LPO@Cu foil. This difference was attributed to defluorination between PVDF and lithium metal, resulting in more LiF forming on the PVDF-LPO@Cu surface. This is beneficial to the formation of a rich-fluoride-containing SEI film, thus improving the stability of the interface.[26]

The fitted F1s spectrum of bare Cu contained two characteristic peaks that were attributed to CF_3 (689 eV) and LiF (684.8 eV). In strong contrast, the spectrum of PVDF-LPO@Cu foil contained an additional characteristic peak of CF_2CF_2 at 687.4 eV, and the CF_2CF_2 content determined from the spectrum was much greater than the original CF_3 and LiF contents.[27,28] Thus, the high-quality fluorine source with a fluorine mass ratio of up to 76% increased the abundance of F atoms on the surface, further ensuring the formation of a fluorinated SEI film.[29] Additionally, in comparison with the XPS image of PVDF-LPO@Cu prior to deposition, the total amount of carbon element did not change significantly. The reason is that the majority of the carbon on the surface of the collector originates from the initial PVDF, and only a small portion comes from the reduction and decomposition of the electrolyte. Unlike C 1s, the F 1s image exhibits additional peaks of CF_3 and LiF. This indicates that the conversion of CF_2 to CF_3 and the reaction with Li^+ occurred during the battery cycle. Combined with the Li 1s diagram of PVDF-LPO@Cu after deposition, it can be proved that the material reacts with lithium ions to form LiF which contributes vitally to the stability of artificial SEI during the cycle process.

Figure 9 shows the electrochemical properties of a copper foil deposited/stripped at a capacity of 0.5 mAh cm^{-2} and a current density of 0.5 mA cm^{-2}.

As shown in Figure 9(a), bare Cu had an initial coulombic efficiency of 79.5%, which increased to approximately 96% in subsequent cycles. However, after the 50th cycle, the coulombic efficiency decreased significantly, decreasing to 81.22% by the 100th cycle. In contrast, the initial coulombic efficiency of PVDF-LPO@Cu was only 55.89%, but this value increased sharply to 98% in subsequent cycles and remained stable. The lower initial coulombic efficiency of PVDF-LPO@Cu compared to that of bare Cu was attributed to the formation of a stable lithium fluoride interface layer upon reaction between lithium metal and PVDF. The stabilized interface layer passivated the lithium-poor surface, caused the unreacted polymer layer to act as a buffer to regulate the deposition and dissolution of lithium, and

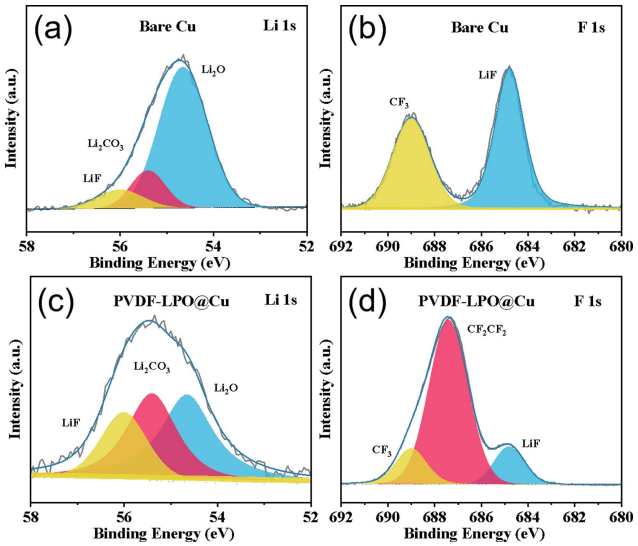

Figure 8. Li 1s and F 1s spectra of bare Cu (a, b) and PVDF-LPO@Cu (c, d) after lithium deposition.

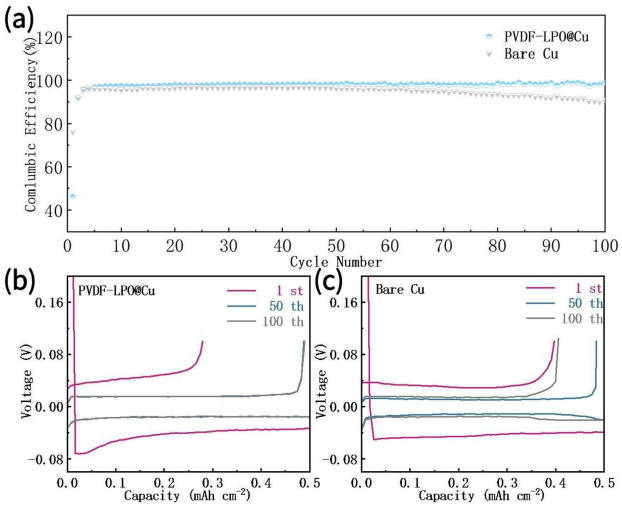

Figure 9. Electrochemical performance of bare Cu||Li and PVDF-LPO@Cu||Li batteries with 1 M LiTFSI dissolved in dimethyl ether and DOL with 2 wt.% $LiNO_3$ as electrolyte

alleviated the stress caused by morphological changes to achieve a stable lithium cycle without dendrite growth. Figure 9(b) and (c) presents the charge and discharge curves of Bare Cu and PVDF-LPO@Cu. It is notable that the initial reversible capacity of Bare Cu was higher than that of PVDF-LPO@Cu, but the value was not stable in the subsequent cycles. In contrast, the charge and discharge curves of the 50th and 100th cycles of PVDF-LPO@Cu almost overlaped, indicating a superior electrochemical stability. Its low initial reversible capacity might be attributed to the reaction of the material with the electrolyte. Under the protection of the PVDF-LPO composite coating, the lithium deposition/dissolution process remains stable and reversible.

Conclusions

To overcome the disadvantages of SEI and dendrite instability stemming from side reactions between metallic lithium and electrolytes, we designed a PVDF-LPO composite coating on a copper foil current collector to prevent the occurrence of these side reactions and the growth of dendrites. The composite coating was prepared by a simple scraping process, allowing good flexibility and stability, and served as a protective layer with excellent mechanical strength and ionic conductivity. In addition, the composite coating effectively minimized the occurrence of interfacial side reactions, allowed homogeneous lithium metal deposition, and restricted the growth of lithium dendrites. The PVDF-LPO@Cu current collector maintained a stable coulombic efficiency of 98% at 0.5 mA cm^{-2} and demonstrated outstanding electrochemical performance when incorporated into full batteries with LFP. To date, researchers have devised detailed improvement strategies to address a series of problems encountered in the commercialization of alkali metals and have made considerable progress. However, the limitations of a singular modification strategy and conflicts between different strategies still hinder the development and application of alkali metals. Future advancements in alkali metals may require a focus on improving artificial SEIs.

Acknowledgements

We acknowledge the funding support from the National Nature Science Foundation of China (No. 52171067), and Guangdong Basic and Applied Basic Research Foundation (No. 2022A1515012366, 2023A1515110792 and 2024A1515010041). The author ANA extends their appreciation to the Deputyship for Research and Innovation, Ministry of Education in Saudi Arabia for funding this research work through the project no. (IFKSUOR3-099-15). We would like to acknowledge the use of facilities in the Analysis and Test Center of Guangdong University of Technology.

Conflict of Interests

The authors declare no conflict of interest.

Data Availability Statement

Data sharing is not applicable to this article as no new data were created or analyzed in this study.

Keywords: Lithium metal anode · Lithiophilic modification · Artificial SEI construction

[1] Y. Cheng, J. Chen, Y. Chen, et al., *Energy Storage Mater.* **2021**, *38*, 276–298.
[2] Y. Lin, Z. Shen, J. Huang, et al., *J. Power Sources* **2023**, *584*, 233612.
[3] Z. Shen, Y. Cheng, S. Sun, et al., *Energy* **2021**, *3*(3), 482–508.
[4] W. Cao, Q. Li, X. Yu, et al., *eScience* **2022**, *2*(1), 47–78.
[5] X. Xie, L. Wei, J. Lu, A. Xu, B. Wang, et al., *Energy Storage Mater.* **2024**, *67*, 103323.
[6] Y. Cheng, Z. Wang, J. Chen, et al., *Angewandte Chemie* **2023**,*135(30)*, e202305723..
[7] Y. Zhong, Y. Chen, Y. Cheng, et al., *Interfaces* **2019**, *11*(41), 37726–37731.
[8] K. Yu, J. Chen, X. Xie, et al., *Surf. Interfaces* **2022**, *34*, 102326.
[9] S. Ye, F. Liu, R. Xu, et al., *Small* **2019**, *15*(46), e1903725.
[10] X. Xie, J. Chen, X. Chen, et al., *J. Electroanal. Chem.* **2023**, *949*, 117862.
[11] M. Fan, Y. Chen, X. Ke, et al., *Sci. China Technol. Sci.* **2022**, *65*(1), 231–237.
[12] A. Willow, H. E. M. Hussein, S. Vajirakaphan, et al., *Front. Energy Res.* **2022**, *10*, 888321.
[13] S. Zhang, Z. Gao, W. Wang, et al., *Small* **2018**, *14*(31), 1801054.
[14] X. Li, G. Yang, S. Zhang, et al., *Nano Energy* **2019**, *66*, 104144.
[15] H. Wu, R. Li, J. Li, et al., *Surf. Inter.* **2024**, *46*, 104048.
[16] Y. Zhou, Y. Han, H. Zhang, et al., *Energy Storage Mater.* **2018**, *14*, 222–229.
[17] C. Duan, Z. Cheng, W. Li, et al., *Energy Environ. Sci.* **2022**, *15*(8), 3236–3245.
[18] J. Luo, C.-C. Fang, N.-L. Wu, *Adv. Energy Mater.* **2018**, *8*(2), 1701482.
[19] S. Hao, Z. Ma, Y. Zhao, et al., *ACS Omega* **2020**, *5*(14), 8299–8304.
[20] J. Luo, R. C. Lee, J. T. Jin, et al., *Chem Commun (Camb)* **2017**, *53*(5), 963–966.
[21] X. Ke, Y. Cheng, J Liu, et al., *ACS Appl. Mater. Interfaces* **2018**, *10*, 13552–1C61.
[22] J. Huang, Z. Shen, S. J. Robertson, et al., *Chem. Eng. J.* **2023**, *475*, 145802.
[23] Q. Fan, S. Yang, J. Liu, et al., *J. Power Sources* **2019**, *421*, 9199.
[24] Z. Shen, J. Zhong, J. Chen, et al., *Chin. Chem. Lett.* **2023**, *34*(3), 107370.
[25] Z. Shen, J. Zhong, S. Jiang, et al., *ACS Appl. Mater. Interfaces* **2022**, *14*, 41022–41036.
[26] Z. Zhou, Y. Feng, J. Wang, et al., *Chem. Eng. J.* **2020**, *396*, 125254.
[27] S. Jiao, J. Zheng, Q. Li, et al., *Joule* **2018**, *2*(1), 110–124.
[28] Y. He, Y. Zhang, P. Yu, et al., *J. Energy Chem.* **2020**, *45*, 1–6.
[29] B. Tong, J. Wang, Z. Liu, et al., *J. Power Sources* **2018**, *400*, 225–231.

Manuscript received: July 5, 2024
Revised manuscript received: August 6, 2024
Accepted manuscript online: August 7, 2024
Version of record online: September 27, 2024